Variable-Density 3D Cones Trajectory Design with Compressed Sensing Reconstruction

Nii Okai Addy[1], Holden H Wu[1,2], and Dwight G Nishimura[1]

[1]Electrical Engineering, Stanford University, Stanford, CA, United States, [2]Cardiovascular Medicine, Stanford University, Stanford, CA, United States

Introduction: The 3D cones trajectory combines aspects of radial and spiral trajectories to efficiently traverse *k*-space. It can provide fast high-resolution imaging with good motion robustness [1]. In an effort to further decrease scan time, undersampling through variable-density trajectory design has been incorporated into other various non-Cartesian trajectories [2-5]. This work introduces a variable-density 3D cones trajectory design method. In addition, a compressed sensing algorithm is used to reduce the presence of aliasing artifacts resulting from the undersampling [6,7].

Methods: The field of view (FOV) is inversely proportional to the *k*-space sampling spacing, hence, the FOV is essentially the sampling density, ρ, of the trajectory. Uniformly increasing the *k*-space sample spacing can create aliasing artifacts. However, an image's spectral content is concentrated near the origin of *k*-space, so reducing the sampling density in the periphery of *k*-space creates a more subtle aliasing artifact.

In 3D cones imaging, the FOV is specified in radial and circumferential components to achieve an anisotropic FOV. The trajectory leaves the origin in a radial direction, then proceeds to oscillate about the k_z-axis along the surface of a cone. In the oscillating segment, if the sampling density is a function of the distance in *k*-space from the origin, k_r, the number of readouts, N, required to satisfy Nyquist requirements on a cone surface at an angle θ_n from the k_z-axis is:

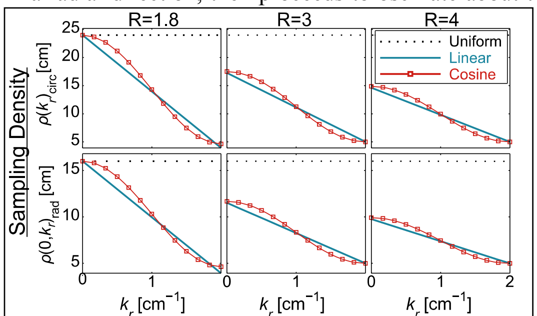

Figure 1: Sampling density functions for R=1.8 (left) R=3 (middle) and R=4 (right).

$$N(\theta_n) = \max_{k_r}\left[2\pi\sin(\theta_n)k_r\left[\left(\frac{G_{circ}(k_r)}{\rho_{rad}(\theta_n,k_r)G_{rad}(k_r)}\right)^2+\frac{1}{\rho_{circ}(k_r)^2}\right]^{-1/2}\right]$$

G_{circ} and G_{rad} are the circumferential and radial trajectory gradients, and ρ_{circ} and ρ_{rad} are the circumferential and radial sampling densities. In the uniform-density case, ρ_{circ} and ρ_{rad} are constant with k_r. $N \propto \rho_{circ}$ and $N \propto \rho_{rad}$ so for a variable-density trajectory, choosing decreasing functions for ρ_{circ} and ρ_{rad} allows imaging at the originally prescribed FOV with fewer readouts, but with some aliasing. The reduction factor R, the ratio of readouts required for a uniform to a variable-density trajectory, is determined by the choice of ρ_{circ} and ρ_{rad}.

A uniform-density trajectory was designed for a 24×24×16 cm^3 FOV, and 1.2×1.2×1.25 mm^3 voxel size, requiring 9217 readouts. This is 36% of the readouts required for an equivalent 3DFT sequence. Three sets of variable-density trajectories were designed with undersampling factors of R = 1.8, 3, and 4. In each set, to test the dependence of aliasing artifacts on the sampling density function, ρ_{circ} and ρ_{rad} were set to linear and cosine functions as shown in Fig. 1. The desired reduction factor was achieved by adjusting the sampling density values at k_r=0 and k_r=k_{max}, then fitting the sampling density function. The readout time was designed for 2 ms for all trajectories. Phantom images were acquired on a 1.5 T GE scanner using a spoiled gradient echo sequence with TE/TR=1/10 ms, 15˚ flip angle and ±125 kHz receiver bandwidth. Reconstruction was performed on a computer with dual 2.6 GHz Xeon x5650 processors and eVGA GTX 580 graphics card. Images were reconstructed using both gridding and a C++/CUDA CS algorithm with total variation regularization, which was run at roughly 5 seconds per iteration for 100, 140, and 200 iterations, for R = 1.8, 3 and 4, respectively, to achieve similar image quality.

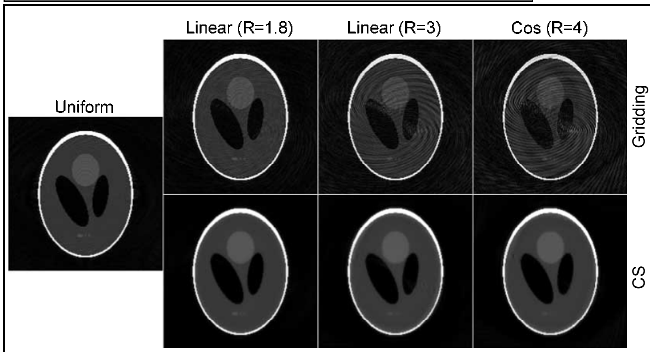

Figure 2: Simulation gridding (top) and CS (bottom) reconstructions for uniform, linear [R=1.8, 3], and cosine sampling densities [R=4].

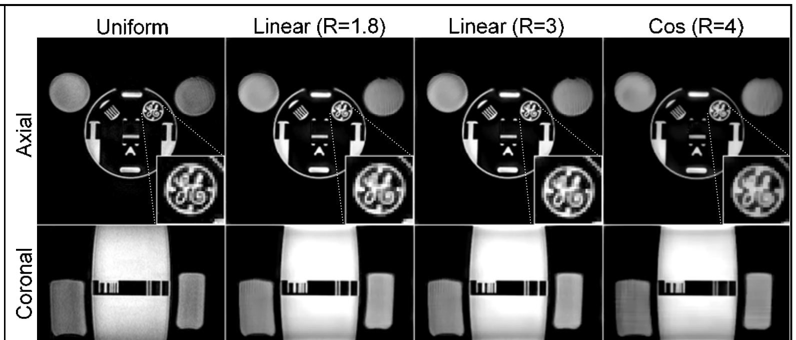

Figure 3: Axial (top) and coronal (bottom) phantom CS reconstructions for linear [R=1.8, 3], and cosine [R=4] sampling densities [R=4]. (Gridding used for uniform)

Results: In simulations, the gridding reconstructions showed moderate aliasing artifacts for R=1.8, and significant aliasing artifacts for R=3 and 4. Comparing CS reconstructions, in the simulated data, of linear vs cosine sampling densities at the same undersampling factor, only small differences in the presence of artifacts could be seen visually (not shown). The linear sampling density at R=1.8 and 3, and the cosine sampling density at R=4, shown in Fig. 2, produced the slight best image quality the respective reduction factors. In the phantom experiments, the CS algorithm does well to remove aliasing artifacts although adding a small amount of blurring, as seen previously in undersampled 3D radial imaging [7]. Reconstructed images closely match the uniform-density case at R=1.8 and 3 with slightly more noticeable residual aliasing artifacts and blurring at R=4.

Conclusion: These initial results show that variable-density 3D cones trajectories can be designed to reduce scan times up to a factor of 11 with respect to 3DFT imaging. With CS reconstruction, images show only slight aliasing artifacts and blurring. More design options exist as the circumferential and radial sampling density functions can individually be designed to create a preferable aliasing pattern. With parallel imaging and randomization of the trajectory, along with optimization of the sampling density functions and CS algorithm, additional scan time reduction and improved image clarity may be possible. Faster CS reconstruction will also be possible with more efficient parallel programming techniques.

References: [1] Gurney, P. PhD Thesis, Stanford University, 2007. [2] Scheffler, K. and Hennig, J. MRM, 40: 474–480, 1998 [3] Lu, A. et al. JMR, 19: 117–23, 2004. [4] Lee, JH. MRM, 50:1276-85, 2003. [5] Pipe, JG. et al. MRM, 66: 1303–1311, 2011. [6] Lustig, M. et al. MRM, 58: 1182–95, 2007. [7] Nam, S. et al. Proc. 19th ISMRM, p. 2548, 2011.